Abstract for The 31st International Workshop on Water Waves and Floating Bodies, Plymouth, Michigan, USA, April 3-6, 2016.

Efficient Modeling of the Free Roll Motion of Ship Hulls with Bilge Keels

Yichen Jiang* **and Ronald W. Yeung**†
Department of Mechanical Engineering
University of California at Berkeley, Berkeley, CA 94720-1740, USA
E-mail: yichen.e.jiang@gmail.com & rwyeung@berkeley.edu

Highlights:

- *Nonlinear time-domain solutions are obtained to accurately predict the free roll motion of a three-dimensional hull with and without forward speed motion in a viscous fluid.*
- *The predicted time histories of the roll motion and the vorticity distribution near a bilge keel are compared with the experimental measurements and the agreements are remarkably good.*

1 INTRODUCTION

A marine vehicle vehicle need to avoid events of capsizing. This is directly connected to its roll-motion and roll-damping properties. Design evaluations of a vessel's roll stability is often a time-consuming process since the roll damping is nonlinear process and viscus in origin. Nonlinearity comes from flow separation and vortex generation arising from hull surface and hull appendages. All these significantly affect the evolution of the roll response.

To predict the roll motion of a ship with bilge keels, a number of theoretical and experimental approaches have been taken. Though the inviscid methods have been widely used in many different applications, its dependence of experimental data to properly fit observation is considered a drawback. Recently, with computer speed improving, computational fluid dynamics (CFD) methods are emerging and show considerable promise (e.g. [1, 2]). However, to achieve high-fidelity simulation, very large number of mesh points is required in such methods. Long-time simulations become very computationally intensive and may not be the best alternative.

Parallel to the CFD development, the discrete-vortex method called Free-Surface Random Vortex Method (FSRVM) was developed at UC Berkeley to study the roll bodies in a viscous fluid (e.g. [3]). These earlier developments, however, were aimed at simulating two-dimensional (2-D) floating bodies, which is in itself a subject of interest [4]. To efficiently simulate the motion of three-dimensional (3-D) hulls, the Slender-Ship Free-Surface Random Vortex Method (SSFSRVM) was developed. A quasi-three dimensional formulation that decomposes the 3-D problem into a number of time-dependent 2-D problems with viscosity present was developed. This 3-D to 2-D conversion for inviscid fluid was proposed by Yeung and Kim [5] in inviscid fluid, but its extension to a viscous fluid was only recently justified [6]. This empowers a scheme that uses the 2-D FSRVM for each ship section, but their solutions are linked. Because SSFSRVM is Lagrangian in formulation, it does not need meshing in the fluid domain, thus not suffering the problem of numerical viscosity. SSFSRVM simulates four degrees of freedom motions: sway, heave, roll, and pitch. The dynamic coupling between fluid motion and body motion presented here is solved by a similar treatment of Seah [7], who considered presecribed or forced motion.

In this abstract, we will examine the effectiveness of SSFSRVM modeling in simulating the free roll decay motion of a ship model with or without forward speed motion. Furthermore, the vorticity distribution near the bilge keels, obtained from the computational model, will be compared with a collection of digital Particle-Image-Velocimetry (DPIV) images from experiments on the same model.

2 THEORETICAL MODEL

2.1 Overview of SSFSRVM

Slender Ship FSRVM (SSFSRVM) takes advantage of the slender-body theory, and simulate the three-dimensional problem of a forward-moving vessel by having the vessel pierce a sequence of stationary (constant χ) planes, as seen in Fig. 1. The transient flow Navier-Stokes solver is carried out in each plane using FSRVM. More information about the governing equations, boundary conditions, and the numerical solutions of the Cauchy integral formula can be found in [6]. In this abstract, the basic formulation of rigid-body motion will be briefly introduced with some details.

*Presenting & Correspondence Author
†Director, Marine Mechanics Lab, UC Berkeley

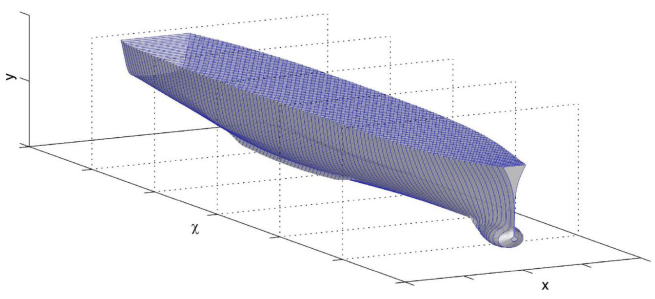

Figure 1: 2-D computational planes along a ship hull.

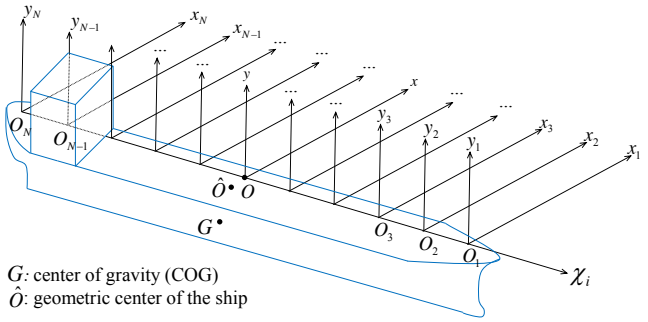

Figure 2: Illustration of the translating coordinate system $O\chi xy$ and its sub-systems spaced evenly on the χ axis.

2.2 Equations of Motion

The equations of motion is set up and solved with respect to the global translating coordinate system ($O\chi xy$ in Fig. 2). We assume the vessel moves with constant forward speed (could be zero) and constant yaw angle. Then, without the surge and yaw accelerations, the 6-DOF equation of motion can be reduced to 4-DOF problem as following:

$$\begin{bmatrix} M_b & 0 & -M_b\check{y}_g & 0 \\ 0 & M_b & M_b\check{x}_g & -M_b\check{\chi}_g \\ -M_b\check{y}_g & M_b\check{x}_g & I_{\chi\chi} & -M_b\check{\chi}_g\check{x}_g \\ 0 & -M_b\check{\chi}_g & -M_b\check{\chi}_g\check{x}_g & I_{xx} \end{bmatrix} \begin{bmatrix} \ddot{x}_b \\ \ddot{y}_b \\ \ddot{\theta}_b \\ \ddot{\gamma}_b \end{bmatrix} = \begin{bmatrix} F_x \\ F_y \\ M_\chi \\ M_x \end{bmatrix} + \begin{bmatrix} M_b\check{x}_g\dot{\theta}_b^2 \\ M_b\check{y}_g(\dot{\theta}_b^2 + \dot{\gamma}_b^2) \\ M_b\check{x}_g\check{y}_g\dot{\gamma}_b^2 \\ -M_b\check{\chi}_g\check{y}_g\dot{\theta}_b^2 \end{bmatrix} \tag{1}$$

where M_b denotes the body mass. $I_{\chi\chi}$ and I_{xx} denote the roll and pitch moments of inertia about the body center $\hat{O}$, respectively. $(\check{\chi}_g, \check{x}_g, \check{y}_g)^T$ denotes the vector from $\hat{O}$ to the center of gravity G. F_x and F_y denote the total external sway and heave forces, respectively. M_χ and M_x denotes the total external pitch and roll moments, respectively.

2.3 Global and Sectional Forces and Moments

By using the slender-ship theory, force and moment contributions from each plane ($O_i x_i y_i$) are combined in a strip-wise manner to obtain the overall force on the vessel. The total external forces and moments acting on the vessel are given as following:

$$\begin{cases} F_x = \sum_{i=1}^{N} F_{1,i} \\ F_y = \sum_i F_{2,i} - M_b g \\ M_\chi = \sum_i F_{3,i} - M_b g\, \check{x}_g \\ M_x = \sum_i F_{2,i} L_i + M_b g\, \check{\chi}_g \end{cases} \tag{2}$$

where $F_{1,i}$, $F_{2,i}$ and $F_{3,i}$ respectively denote the lateral force, vertical force, and roll moment acting on the i-th station. Apart from the first equation, showing the limits of the summation over i, we will henceforth adopt the simplified notation of $\sum_i$ to mean the same limits of i. The sectional loads can be obtained by integrating the pressure over the wetted sectional body contour, girthwisely.

Following [7], we can obtain the total hydrostatic and hydrodynamic forces and moment acting on the $i-th$ section (the $O_i x_i y_i$ plane in Fig. 2) with respect to the corresponding translating frame of reference will be as following:

$$\begin{cases} F_{1,i} = (A_{41,i} - A_{11,i}\ddot{x}_{\hat{O}_i} - A_{12,i}\ddot{y}_{\hat{O}_i} - A_{13,i}\ddot{\theta}_{\hat{O}_i})\Delta L \\ F_{2,i} = (A_{42,i} - A_{21,i}\ddot{x}_{\hat{O}_i} - A_{22,i}\ddot{y}_{\hat{O}_i} - A_{23,i}\ddot{\theta}_{\hat{O}_i})\Delta L \\ F_{3,i} = (A_{43,i} - A_{31,i}\ddot{x}_{\hat{O}_i} - A_{32,i}\ddot{y}_{\hat{O}_i} - A_{33,i}\ddot{\theta}_{\hat{O}_i})\Delta L \end{cases} \tag{3}$$

where $A_{jk,i}, j, k = 1, 2, 3$ represent the sectional hydrodynamic added mass or moment of inertia; $A_{4k,i}, k = 1, 2, 3$ are the rest forces or moment acting on the section. ΔL denotes the distance between two neighboring sections.

By using these coefficients, the final 4-DOF equations of motion with respect to the global translating frame can be expressed as:

$$\begin{bmatrix} B_{11} + M_b & B_{12} & B_{13} - M_b\check{y}_g & -B_{14} \\ B_{21} & B_{22} + M_b & B_{23} + M_b\check{x}_g & -B_{24} - M_b\check{\chi}_g \\ B_{31} - M_b\check{y}_g & B_{32} + M_b\check{x}_g & B_{33} + I_{\chi\chi} & -B_{34} - M_b\check{\chi}_g\check{x}_g \\ -B_{41} & -B_{42} - M_b\chi_g & -B_{43} - M_b\check{\chi}_g\check{x}_g & B_{44} + I_{xx} \end{bmatrix} \begin{bmatrix} \ddot{x}_b \\ \ddot{y}_b \\ \ddot{\theta}_b \\ \ddot{\gamma}_b \end{bmatrix} = \begin{bmatrix} W_{41} + M_b\check{x}_g\dot{\theta}_b^2 \\ W_{42} + M_b\check{y}_g(\dot{\theta}_b^2 + \dot{\gamma}_b^2) - M_b g \\ W_{43} - M_b g\check{x}_g + M_b\check{x}_g\check{y}_g\dot{\gamma}_b^2 \\ -W_{44} + M_b g\check{\chi}_g - M_b\check{\chi}_g\check{y}_g\dot{\theta}_b^2 \end{bmatrix} \tag{4}$$

where the coefficients B_{jk} and W_{jk} can be formally defined as:

$$\begin{cases} B_{jk} = \sum_i A_{jk,i}\Delta L, & j,k = 1,2,3 \\ B_{j4} = \sum_i A_{j2,i} L_i \Delta L, & j = 1,2,3 \\ B_{4k} = \sum_i A_{2k,i} L_i \Delta L, & k = 1,2,3 \end{cases} \quad \& \quad \begin{cases} W_{4j} = \sum_i A_{4j,i}\Delta L, & j = 1,2,3 \\ B_{44} = \sum_i A_{22,i} L_i^2 \Delta L \\ W_{44} = \sum_i A_{42,i} L_i \Delta L \end{cases} \tag{5}$$

Equation (4) completely describes the dynamic coupling between the fluid and body, which can be solved explicitly to yield $(\ddot{x}_b, \ddot{y}_b, \ddot{\theta}_b, \ddot{\gamma}_b)$ at any given time, t.

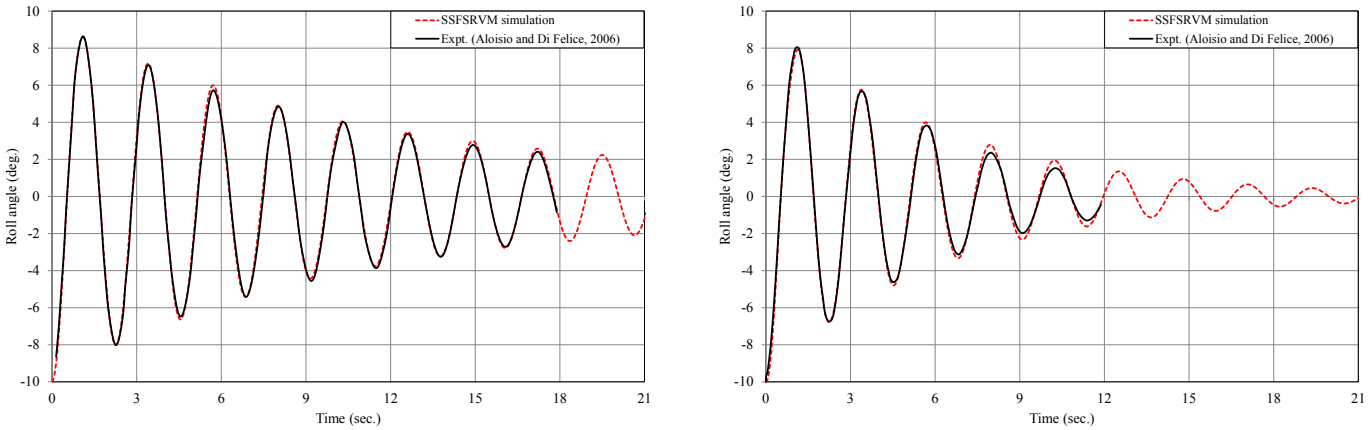

(a) Zero speed case, $Fr = 0$ (b) Forward speed case, $Fr = 0.138$

Figure 3: Comparison of the roll motion between the experimental measurement and the SSFSRVM simulation .

With the body acceleration having been solved as described, the velocity and displacement can be integrated in time to advance the position of the body. Then the kinematic and dynamic conditions are used to update the boundary nodes. A new set of boundary conditions is available for the next time step. The time-domain simulation with free motion is now accomplished.

3 RESULTS

Aloisio & Felice [8] conducted an experimental study of the velocity field around a ship model (DTMB-5415, 5.7m length) in free roll decay motion at the INSEAN towing tank. The flow around the bilge keels was investigated using a 2-D PIV underwater system. Their experiments visualize the fluid dynamics and provide a set of certified experimental data for validating our numerical method. The comparison of the time histories of roll decay motion from the experiments and SSFSRVM simulations is presented in Fig. 3, for a zero forward-speed case, as well as a forward-speed case of Froude number Fr=0.138. It can be seen that the predicted time history matches exceedingly well with the experimental data, a remarkable confirmation of the present theory.

Figure 4 illustrates the capability of SSFSRVM to predict the bilge-keel vorticity evolution at the longitudinal location χ, being 50.4% from the bow at zero forward speed. This is compared with the corresponding time instants of PIV measurements. The vorticity color scales are identical for both plots. It is observed, from both PIV measurements and simulation, a pair of counter-rotating vortices is generated and convected away from the bilge keel when the roll motion changes directions. The distances that the vortex pair travels are predicted closely by the numerical method. Though minor differences can be found in the comparison, we consider the model to be capturing the motion of the vortical structures well.

Figure 5 presents the vorticity evolution at the longitudinal location $\chi/L = 0.675$ for the forward speed of Fr=0.138. Remarkable agreement in the core size and core strength between the simulations and the measurements is seen. These results, being with forward speed, have cumulative convective effects from upstream, lending credence to the SSFSRVM formulation for three-dimensional ship flow.

Based on the above comparisons of roll-motion time histories and vorticity evolution, we see that SSFSRVM is able to simulating free-decay motion of a model with and without forward speed. Such free-decay motion is often used to obtain experimental roll damping. In effect, SSFSRVM provides us a successful numerical wave-tank test.

The results for 10 cycles of roll motion took 6 hours on a standard desktop computer with an Intel Core i7-4770 processor. It is a very effective predictive tool.

In addition, SSFSRVM can also be applied to simulate the ship motion in beam waves. An oscillating pressure patch is used to generate regular incident waves on the starboard-side free surface with the wave height of 2.48 cm, and the wave period of 2.25 s. Figure 6 shows the roll responses of four ship models with the same DTMB-5415 hull form but different bilge keel spans. Through the comparison of the responses, it can be seen that increasing the bilge keel size decreases the roll amplitude and increases the roll period. Compared to the BK0 model, the motion amplitudes of the BK1, BK2, and BK3 models are reduced by 6%, 11%, and 32%, respectively.

References

[1] Wilson, R.V., Carrica, P.M., and Stern, F. (2006), *Computers & Fluids*, Vol.35 (5), pp. 501-524.

[2] Miller, R., Bassler, C., Atsavapranee, P., and Gorski, J. (2008), *Proceedings of the 27th Symposium on Naval Hydrodynamics*, Seoul, South Korea.

[3] Yeung, R.W., 2002, Plenary Paper, *Proc.* Int'l Society of Offshore and Polar Engineers (ISOPE), Vol. 3, pp. 1-11.
[4] Jiang, Y. and Yeung, R. W. (2015), Journal of Offshore Mechanics and Arctic Engineering, Vol. 137(6), 061901.
[5] Yeung, R.W. and Kim, S.H. (1981), *Proc.*, 3rd Int'l Conf. on Numerical Ship Hydrodyn., Paris, France.
[6] Yeung, R.W., Seah, R.K.M. and Imamura J.T. (2013), *J. Offshore Mech. Arct. Eng.*. 135(3), 031101.
[7] Seah, R.K.M., Celano, T. and Yeung, R.W. (2002), *Proc.*, 17th IWWWFB, Cambridge, England.
[8] Aloisio, G., and F. Felice. (2006), *XIV Congresso Nazionale AI VE. LA.*, Rome, Italy.

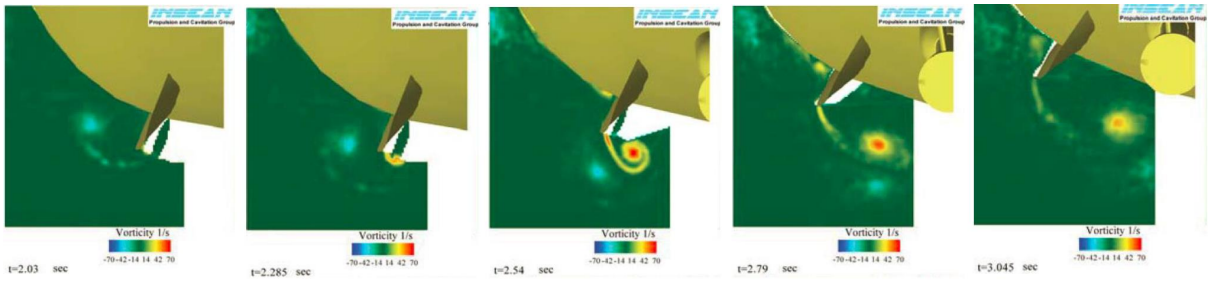

(a) Experimental measurements.

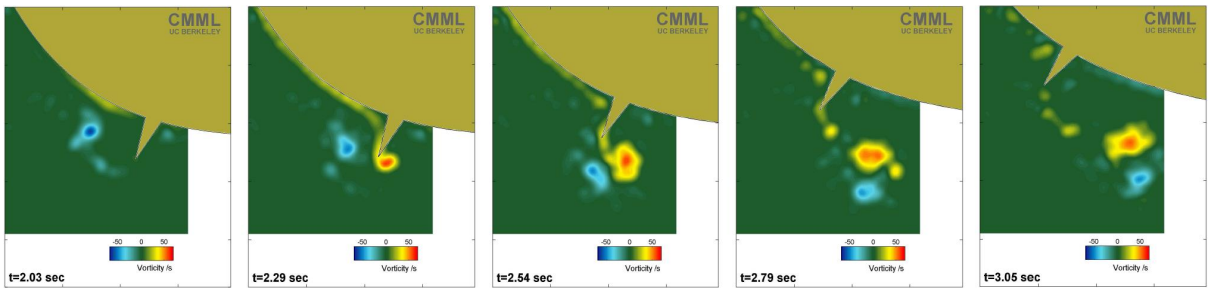

(b) SSFSRVM simulations.

Figure 4: Comparisons of vorticity evolution between experiments and simulations (t=2.03 to 3.05 sec, and $Fr = 0$).

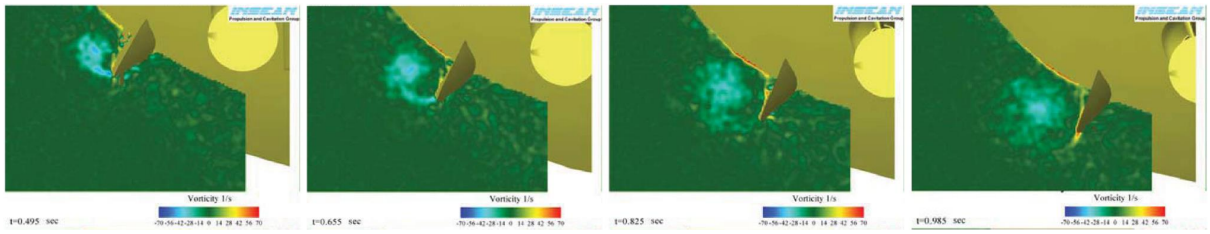

(a) Experimental measurements.

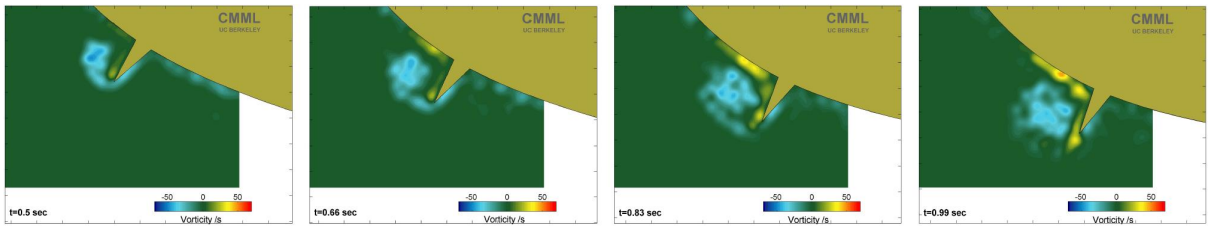

(b) SSFSRVM simulations.

Figure 5: Comparisons of vorticity evolution between experiments and simulations (t=0.50 to 0.99 sec, and $Fr = 0.138$).

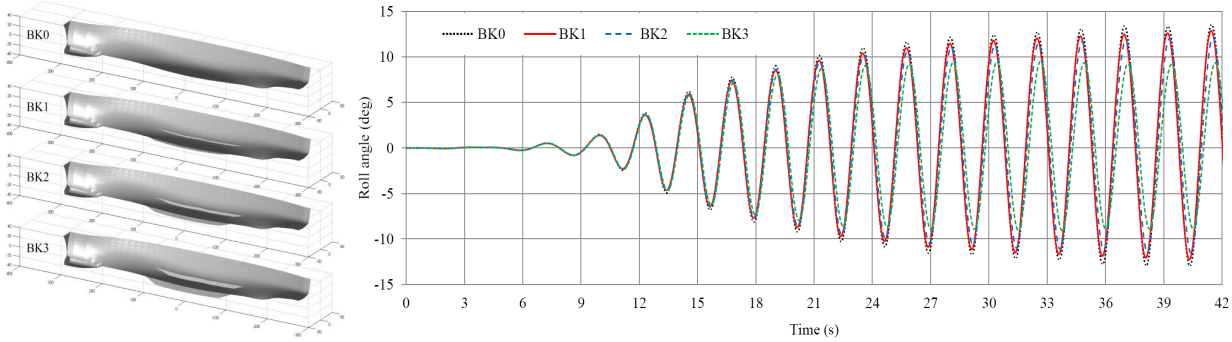

Figure 6: Comparison of the time histories of the roll response in waves between hulls with different bilge keel configurations.